

## Comparison of cold season sedimentation dynamics in the non-tidal estuary of the Northern Baltic Sea

Jouni Salmela<sup>a,\*</sup>, Saija Saarni<sup>a,b</sup>, Linnea Blåfield<sup>a</sup>, Markus Katainen<sup>c</sup>, Elina Kasvi<sup>a,d</sup>, Petteri Alho<sup>a,e</sup>

<sup>a</sup> University of Turku, Department of Geography and Geology, FI-20014 Turun yliopisto, Finland

<sup>b</sup> University of Helsinki, Faculty of Biological and Environmental Sciences, PL 65, 00014 Helsinki, Finland

<sup>c</sup> Sitowise Oy, Helsinginkatu 15, FI-20500 Turku, Finland

<sup>d</sup> Turku university of Applied Sciences, Joukahaisenkatu 3, FI-20520 Turku, Finland

<sup>e</sup> Finnish Geospatial Research Institute, Geodeetinrinne 2, FI-02430 Masala, Finland

### ARTICLE INFO

#### Keywords:

Sedimentation rate  
Hydrodynamic modelling  
Sediment trap  
Sediment characteristics  
Flow dynamics  
Cold season  
Baltic Sea

### ABSTRACT

In this study, we investigated sedimentation differences between two distinctive cold seasons, in terms of hydrometeorological and hydrodynamic conditions, in a coastal area of the Northern Baltic Sea in 2018–2020. A combination of sediment trap data, hydrometeorological data and hydrodynamic modelling provided a unique set-up to discover differences in sedimentation rates and compositions. Our study shows that the averaged sedimentation accumulation rate (SAR) was nearly three times higher during warmer cold season ( $30.9 \text{ g m}^{-2} \text{ day}^{-1}$ ), characterised by higher precipitation, especially rain and discharge, as well as snowless and open water conditions, compared to regular cold season ( $10.6 \text{ g m}^{-2} \text{ day}^{-1}$ ). While sedimentation was higher during the warmer season, the mean sediment grain size ( $D_{50}$ ) was higher during the regular cold season with permanent snow and ice cover. Similarly, while sediments of the regular cold season were organically rich, the total amount of organic matter accumulation was larger during the warmer cold season. Sediments consisted mostly of clastic matter (85–89%), of which the mean grain size varied from clay to fine silt ( $0.3\text{--}3.0 \mu\text{m}$ ). Sedimentation differences between the cold seasons can be explained by differences in precipitation, river flow, wind-induced resuspension and a low air pressure system forcing sea level changes. Sedimentation differences along the study bay were found to be connected to channel cross-sectional area and flow conditions caused by river input and sea level changes.

### 1. Introduction

Due to the climate change, precipitation and temperature are predicted to increase (Ruosteenoja and Jylhä, 2007), and the discharge regime in coastal Finland is estimated to change (Veijalainen et al., 2010). Warming and precipitation increases are estimated to be strongest during winters (Ruosteenoja and Jylhä, 2007), which will most likely enhance the sediment yields from watersheds to water basins, especially outside the vegetation period when soil is more prone to erosion. Increased sediment concentration in water bodies reduces light penetration, and thus, primary production (Pedersen et al., 2012) and increased sedimentation rates have been recorded to smother benthic fauna (Chou et al., 2004). In addition, the duration of ice cover during the winter season is estimated to decrease in the Baltic Sea region

(Jevrejeva et al., 2004; Vihma and Haapala, 2009), exposing shorelines for longer periods of erosion (Ryabchuk et al., 2011).

The Baltic Sea is an enclosed non-tidal, brackish-water-dominated shallow sea, in which multiple factors, such as wind, river discharge, and ice cover, control sedimentation. Wind-induced mixing during storm events causes higher bottom turbidity rates, and consequent resuspension (Rasmus et al., 2015). Previous research has shown enhanced sedimentation on relatively shallow water related to wind-induced resuspension (Christiansen et al., 2002; Lund-Hansen et al., 1999; Nuorteva and Kankaanpää, 2016). In the vicinity of river mouths, the sedimentation has been found to be higher compared to the sedimentation offshore (Chubarenko et al., 2019; Kankaanpää et al., 1997; Szymkiewicz and Zalewska, 2014).

In the Northern Baltic Sea region, coastal areas are typically ice-

\* Corresponding author.

E-mail address: [jouni.jsalmela@utu.fi](mailto:jouni.jsalmela@utu.fi) (J. Salmela).

<https://doi.org/10.1016/j.margo.2021.106701>

Received 2 July 2021; Received in revised form 16 October 2021; Accepted 28 November 2021

Available online 6 December 2021

0025-3227/© 2021 The Authors. Published by Elsevier B.V. This is an open access article under the CC BY license (<http://creativecommons.org/licenses/by/4.0/>).

covered during the winter season (mid-December–end of March). Ice cover isolates the water from atmospheric action, hindering wind-driven mixing (Merkouriadi and Leppäranta, 2015) and wave action (Ryabchuk et al., 2011). Sedimentation studies of ice cover conditions in coastal areas of the Baltic Sea have been recorded mainly by lagoon studies (Chubarenko et al., 2019), highlighting rivers as a single-sediment sources during the ice cover period. Comparative sedimentation studies between ice cover and open water conditions in seasonal ice covered lakes have found higher sedimentation resuspension rates under ice-free than ice-cover conditions (Kleeberg et al., 2013; Niemistö and Horppila, 2007). Studies highlighted that shortening ice-cover duration in predicted warmer climate will increase sediment resuspension in lake environments.

In addition to meteorological conditions, sediment grain size and composition, as well as flow conditions, define sedimentation processes. Larger sediment particles accumulate closer to the particle source due to higher settling velocity. In addition, smaller particles may aggregate, resulting in larger particle sizes and, thus, higher settling velocities. Despite the clear link of sedimentation processes and hydrodynamic conditions, studies combining hydrodynamic modelling and sediment trapping in boreal regions are rare.

In the southern region of the Baltic Sea, sedimentation has been recorded to be highest during autumn–winter period (Szymkiewicz and Zalewska, 2014). However, comparison of cold season sedimentation dynamics in high latitude zones, with typically strong variation in terms of precipitation, as well as ice and snow cover conditions, are rare. For example, many sedimentation studies related to annual sedimentation have been conducted in the Baltic Sea region (Eckh ell et al., 2000; Jokinen et al., 2015; Kankaanp aa et al., 1997; Suplinska and Pietrzak-Flis, 2008). These studies mainly describe annual sedimentation excluding inter-annual behaviour. Annual sediment accumulation rate (SAR) in the Baltic Sea region shows large variations between coastal and open sea areas, with the highest SAR documented in the gulf areas (Suplinska and Pietrzak-Flis, 2008). The average sedimentation rate in the coastal areas has been estimated at 317–543 g m<sup>-2</sup> yr<sup>-1</sup>, and 108–273 g m<sup>-2</sup> yr<sup>-1</sup> in the deep areas, in the southern Baltic Sea region (Suplinska and Pietrzak-Flis, 2008). Kankaanp aa et al. (1997) recorded a 1500 g m<sup>-2</sup> yr<sup>-1</sup> mean accumulation rate for the Gulf of Finland, which underlines the higher sedimentation rate in the coastal areas than open sea areas.

The aim of this study is to compare sedimentation and sedimentation processes between two different cold seasons, in terms of ice and snow cover, precipitation and flow conditions. We combine sediment characteristics, hydrometeorological conditions and hydrodynamic modelling to detect both seasonal and areal sedimentation differences, and to find relationships between sedimentation and flow conditions. To our knowledge, combining hydrodynamic modelling and sedimentation data is still rare, and it may provide new insights into coastal sedimentation processes. We focused on SAR, sediment characteristics and grain size, carbon and nitrogen contents, and their ratio (C/N). We are seeking answers to the following research questions.

- 1) How sedimentation varies between two cold seasons with very different conditions?
- 2) What causes the differences in sedimentation?

## 2. Regional setting

We performed our study in Halikonlahti Bay, located at the Archipelago Sea, Baltic Sea (Fig. 1). Halikonlahti Bay forms an enclosed estuary for the Uskelanjoki and Halikonjoki Rivers, with two openings to the Archipelago Sea separated by Kemi onsaari Island. Both channels are more than 40 km long and depth along the study channel thalweg varies between shallow (<5 m) and deeper (>20 m) parts (Fig. 1). The mean discharge of Uskelanjoki River is 5.0 m<sup>3</sup> s<sup>-1</sup> (in 1971–2020), and the Halikonjoki River discharge has been estimated as approximately 57% of the discharge of the Uskelanjoki River (HERTTA database, 2021). The

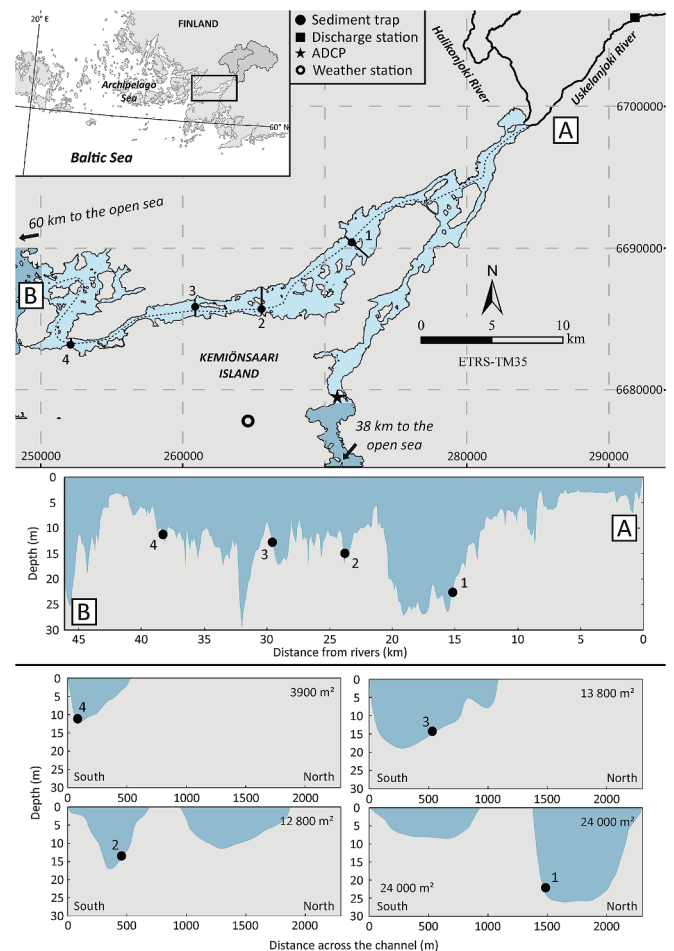


**Fig. 1.** The study area and the locations of sediment traps. Drainage areas for Uskelanjoki and Halikonjoki Rivers are shown in inset map. Hydrodynamic model domain is indicated with light blue. The vertical locations of the sediment traps are shown in the bathymetric transect and channel cross-sections, including cross-sectional areas. (For interpretation of the references to colour in this figure legend, the reader is referred to the web version of this article.)

discharge between May and September is generally low (mean discharge 2.3 m<sup>3</sup> s<sup>-1</sup>), while most of the river discharge occurs between October and May (mean discharge 6.8 m<sup>3</sup> s<sup>-1</sup>). The highest discharge peaks typically occur during the snowmelt period between March and April. Sea level fluctuations in Baltic Sea and Archipelago Sea are mainly forced by passages of low air pressure systems. Salinity varies between 0 and 6 PSU in the study area. Between October and April, the water temperature remains below 10 °C, and neither the thermo- nor halocline occur due to the shallowness of the bay. In this study, we focused on the cold season, September/October–May, which is characterised by the higher river flow and, typically, the sea ice cover in order to understand the influence of the warmer winter conditions predicted for the future.

The catchment area of the two rivers is heavily cultivated, with 36% non-irrigated arable land. The soil type is 59% of clay and 21% of bedrock or bare rock. The catchment area is the former sea bottom, which has uplifted from the sea due to post-glacial rebound, ca. 5 mm yr<sup>-1</sup> (Eronen et al., 2001).

Owing to the enclosed character of the Halikonlahti Bay, the average fetch length for the study area is less than 2 km (Tolvanen and Suominen, 2005). Steep banks and gently sloping fields surround the bay. Our study focused on the western channel with a 0.25–3.3-km channel width (Fig. 1).

### 3. Materials and methods

#### 3.1. Meteorological data

We based our study on sedimentation data collected during two consecutive cold seasons in 2018–2020. To perform our analysis, we derived data for precipitation, snow cover, and wind conditions from the national weather station (Kemiönsaari Kemiö, 100951), maintained by Finnish Meteorological Institute (FMI). The weather station is located in an open field on Kemiönsaari Island, approximately 10 m above sea level within 8 km distance to the study channel (Fig. 1).

#### 3.2. Hydrodynamic modelling

To evaluate the characteristics of the flow fields in the Halikonlahti Bay, a three-dimensional hydrodynamic model was created (see model domain in Fig. 1). The effect of river discharges variation and sea level fluctuations on flow conditions were simulated with Delft 3D. The model consists of a curvilinear grid with cell size variations of 31–80 m in the horizontal direction. In a vertical direction, the grid contains six layers with cell sizes of 10%, 15%, 15%, 20%, 20%, and 20% of the water column from the surface to the bottom, respectively. Smaller vertical cell sizes near the surface were selected to distinguish the possible development of the buoyant river plume described by Salmela et al. (2020). The geometry of the hydrodynamic model is based on the Coastal Terrain Model of the Archipelago Sea (2009), with 5 m resolution, produced by Department of Geography and Geology, University of Turku. Both discharges of the Uskelanjoki and Halikonjoki Rivers were used to calculate hourly inflow to the bay as upstream boundary conditions. The Finnish Environment Institute (SYKE) provided the data from the Uskelanjoki River, and the Halikonjoki River discharge was calculated based on the discharge of the Uskelanjoki River. The discharge gauging station (Kaukolankoski, 2500400) of the Uskelanjoki River is located ca. 13 km upstream from the river mouth (Fig. 1).

Sea levels were selected for the downstream boundary conditions. Sea levels were interpolated based on two national mareograph stations maintained by FMI: Turku Ruissalo Saaronniemi (134225) and Hanko Pikku Kolalahti (134253) at ca. 30 km and 40 km distance from the study area, respectively. Salinity values of 0 and 5 PSU were nominated for river input and sea water boundary conditions, respectively (see detailed water quality measurements, Salmela et al., 2020).

Hydrodynamic model was calibrated by adjusting Manning's roughness value and modelling time step. For the best model results, a Manning's roughness value of 0.02 and a time step of 0.5 min were selected. The model was validated using five-day flow data (Fig. 2), collected and administered by Finnish Transport Infrastructure Agency in Strömma Strait with Acoustic Doppler Current Profiler (SonTek-SL

Series) (see location in Fig. 1). Flow values were measured from the mid water, and modelled values are depth-averaged velocities.

Final model with hourly interval was based on combined inflow of the Uskelanjoki and Halikonjoki Rivers and sea level at the end of both channels as open boundary conditions. The modelling periods were the 210 (10.10.2018–7.5.2019) and 233 days (18.9.2019–7.5.2020). The modelled hourly flow velocities at trap locations were extracted for the final analyses (Figs. 6 & 7) and surface and bottom flow velocities were selected for closer inspection (Table 1).

#### 3.3. Sedimentation

Sedimentation was monitored with four bottom-mounted sediment traps equipped with two freely movable plastic funnels with a diameter of 62 mm, height 405 mm (Fig. 3). In this study, only the sediment from a single funnel was analysed, and sediment from the other funnel was stored for further studies. The traps were equipped with two floaters and installed at 1.5 m above the sea bottom. This measurement setup was selected on the basis of earlier sediment studies (Horppila and Niemistö, 2008; Ojala et al., 2013). The trap locations were based on channel depth, distance from the river mouths, and bottom type: traps were installed in bathymetric depressions and expected accumulation zones, but avoided the fairways (Fig. 1). The sediment traps were deployed during autumn and collected on spring. The duration of the data collection was 210 (10.10.2018–7.5.2019) and 233 days (18.9.2019–7.5.2020) for the first and second cold season, respectively.

Sediment samples were collected by rinsing the funnels with deionised water into 3-L lidded containers and stored at 5 °C for further analyses. At the laboratory, water was decanted away, and the sediments were dried at 60 °C for 48 h. The sediment sample dry weight was measured, and the sediments were homogenised using agate mortar. Subsamples were taken to evaluate the sediment's organic matter content, organic matter sources, and grain size distribution. The SAR ( $\text{g m}^{-2} \text{day}^{-1}$ ) was calculated from sample dry weights.

Organic matter (OM) content was measured using the loss on ignition (LOI) method (Heiri et al., 2001), in which 0.5 g of dry sediment powder was combusted at 550 °C for 4 h. Samples were cooled in an exicator prior weighing. The OM content was measured through the LOI from combusted samples, while siliciclastic minerogenic matter (MM) was obtained subtracting OM from the total sample weight.

The total carbon and total nitrogen content were analysed from bulk sediments using thermal combustion. Approximately 2.5 mg of homogenised and dried sediment powder was weighed into a tin cup, which was then analysed using a CHN-900 analyser (Leco TruSpec Micro, US) with  $\pm 0.001\%$  and  $\pm 0.01\%$  accuracy for carbon and nitrogen, respectively. Inorganic C and N are negligible in this type of setting (Jilbert et al., 2018) and hence total C and N represent organic C and N.

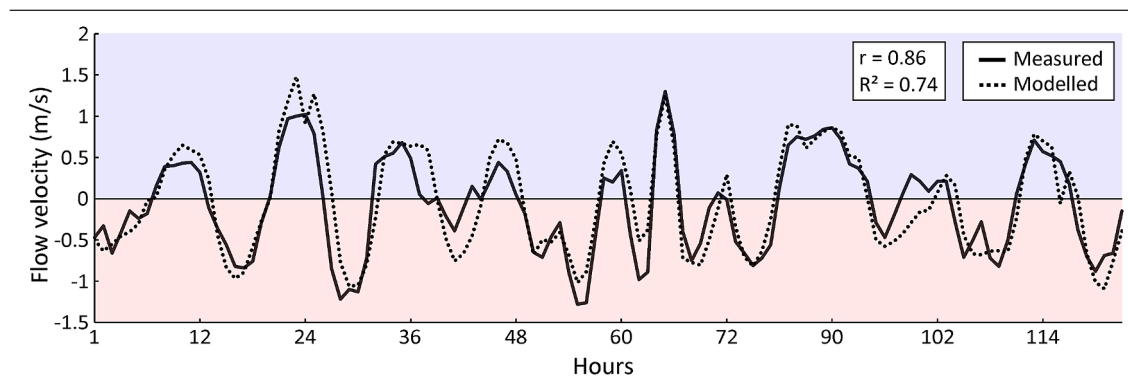


Fig. 2. Validation of the hydrodynamic model based on flow measurements conducted in Strömma strait (see location in Fig. 1). Positive (blue background) and negative (red background) values indicate out- and inflow from the Halikonlahti Bay, respectively. Statistical characteristics  $r$  and  $R^2$  describe the quality of the hydrodynamic model. (For interpretation of the references to colour in this figure legend, the reader is referred to the web version of this article.)



**Table 1**  
Details of data collection sites, flow conditions and sediment data from each trap in both seasons.

Trap	4		3		2		1		
Cross-sectional area (m <sup>2</sup> )	3900		13,800		12,800		24,000		
Distance from river mouths (km)	37.4		28.5		23.4		15.5		
Season	1st	2nd	1st	2nd	1st	2nd	1st	2nd	
Trapping period (days)	210	233	210	233	210	233	210	233	
Mean river discharge (m <sup>3</sup> s <sup>-1</sup> )	5.1	9.7	5.1	9.7	5.1	9.7	5.1	9.7	
Surface flow velocity (cm s <sup>-1</sup> )	Average	6.4	8.5	3.1	3.8	3.0	3.7	2.5	3.0
	Min	0.0	0.0	0.0	0.0	0.0	0.0	0.0	0.0
	Max	45.2	60.4	16.6	22.8	15.9	23.3	8.8	12.5
Bottom flow velocity (cm s <sup>-1</sup> )	Average	5.0	5.8	1.7	2.1	2.2	3.0	1.0	1.2
	Min	0.0	0.1	0.0	0.0	0.0	0.0	0.0	0.0
	Max	30.3	47.1	11.0	14.6	10.9	17.4	4.4	6.3
Dry mass of trapped material (g)	4.6	31.5	4.4	10.3	9.6	18.1	4.7	15.8	
SAR (g m <sup>-2</sup> day <sup>-1</sup> )	8.4	51.4	8.0	16.8	17.4	29.5	8.5	25.8	
SAR minerogenic matter (g m <sup>-2</sup> day <sup>-1</sup> )	7.2	46.0	6.9	14.7	14.9	25.8	7.2	22.5	
SAR organic matter (g m <sup>-2</sup> day <sup>-1</sup> )	1.2	5.4	1.2	2.1	2.4	3.7	1.2	3.3	
Minerogenic matter (%)	86.0	89.6	85.7	87.4	86.0	87.6	85.4	87.2	
Organic matter (%)	14.0	10.4	14.3	12.6	14.0	12.4	14.6	12.8	
C/N	10.42	10.32	11.28	10.51	10.93	10.10	11.12	11.72	
D <sub>50</sub> grain size (µm)	2.554	3.231	0.616	0.476	1.200	0.416	0.670	0.354	



**Fig. 3.** Two funnel sediment trap with floaters (A) and a funnel containing sediment sample (B) after a trapping period.

Approximately 1.0 g samples were weighed into 50-ml glass beakers for the grain size analyses. Samples were pretreated with 33% H<sub>2</sub>O<sub>2</sub> at 80 °C to remove organic material, followed by boiling with 8% NaOH in order to remove diatoms. Mineral grain sizes were analysed using a Mastersizer 2000 (Malvern Panalytical Ltd).

## 4. Results

### 4.1. General characteristic of seasons and river discharge

During the first cold season, the mean discharge was 5.1 m<sup>3</sup> s<sup>-1</sup>. Discharge remained mainly low from the beginning of the trapping period until the middle of February, except in the middle of December when discharge exceeded 20 m<sup>3</sup> s<sup>-1</sup> (Fig. 4). The highest flow event was recorded at the end of March with 50 m<sup>3</sup> s<sup>-1</sup> discharge. Discharge peaks from the middle of February onwards were linked to snowmelt and increased rainfall. Based on satellite images, the bay was covered in ice between approximately December 14 until April 1 (109 days), and most of the flow (75%) occurred during the ice cover period (Fig. 5). However, there was a great variation in the duration of ice cover along the bay. The mean temperature in the winter months (DJF) was -2.0 °C. Furthermore, the first season was characterised by permanent snow cover at the catchment area from middle December until the middle of

March (95 days) (Fig. 4). The average precipitation and wind speed for the first season was 1.7 mm and 3.4 m s<sup>-1</sup>, respectively.

Second cold season was characterised by open water and snowless conditions (Figs. 4 & 5), with a mean temperature of 2.2 °C (DJF), 4.2 °C warmer than the first season. While the mean discharge for the first season was 5.1 m<sup>3</sup> s<sup>-1</sup>, for the second season it was nearly two times higher (9.7 m<sup>3</sup> s<sup>-1</sup>). Daily average precipitation for the second season was 2.86 mm, which was 1.7 times higher compared to the first season. During high rainfall events, the discharge of Uskelanjoki River rose over 20 m<sup>3</sup> s<sup>-1</sup> several times (Fig. 4). The peak discharge value (> 100 m<sup>3</sup> s<sup>-1</sup>) was recorded in the middle of February after a heavy rainfall event. The average wind speed for the second season was 4.0 m s<sup>-1</sup>, which was 0.6 m s<sup>-1</sup> higher compared to the first season.

### 4.2. Hydrodynamic conditions

Our hydrodynamic models show that the high flow velocity events in the Halikonlahti Bay occur during river discharge peaks and sea level changes (Figs. 6 & 7, highlights A and B). The second season was more active in terms of flow velocities (Table 1). At each trap location both the average surface and bottom flow velocities were higher during the second season. The average surface flow velocity was more than two times higher at trap 4 than traps 1–3 during both seasons. A similar



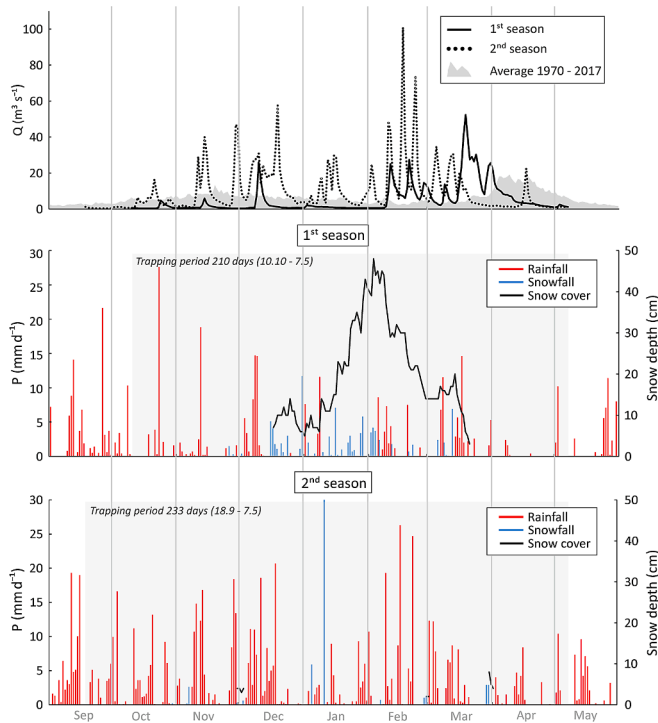


**Fig. 4.** Hydrographs for the Uskelanjoki River with precipitation (P) (rain- and snowfall) and snow cover for the study area. Trapping periods are highlighted for both seasons with a light grey background.

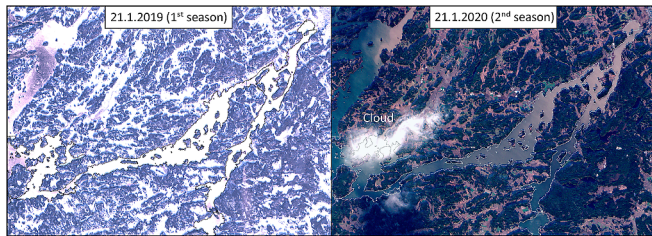


**Fig. 5.** Sentinel satellite images showing the snow and ice cover conditions during both seasons. While the first season is characterised by permanent snow and ice cover, the second season lacks snow and ice cover. The dark areas in both images are mainly tree canopy, and the brighter areas are arable land. Turbid water can be seen near the river mouth during the second season. The shoreline is highlighted for better visualisation in both images.

difference was found in averaged bottom velocities. In addition, the highest flow velocities up to  $45 \text{ cm s}^{-1}$  and  $60 \text{ cm s}^{-1}$  for the first and second seasons, respectively, were located at trap 4.

While the highest flow velocity events at traps 1–3 (up to  $16 \text{ cm s}^{-1}$ ) occurred during snowmelt-enhanced spring floods (Fig. 6, highlights A) during the first season, the highest flow velocity events during the second season were distributed for the entire trapping period (Fig. 7). Interestingly, the flow profile at trap 1 had two high velocity cores: at the surface 1–5 m depth and middle layer at 5–10 m depth (Figs. 6 & 7, highlight A) while at traps 2–4, high velocity cores were located also next to the bottom, especially during the second season.

Based on correlation analysis, the highest correlations between river discharge and surface flow velocities, 0.46 and 0.39 for the first and second seasons, respectively, were found at trap 1, closest to the river mouths (Table 2). For bottom flow velocities, the highest correlation was found at trap 1 (0.24) and 3 (0.27) for the first and second seasons, respectively. The highest correlation (0.31) between sea level changes and surface flow velocities were found closest to the open sea, at trap 4, during both seasons. Similarly, the highest correlation, 0.34 (1st season)

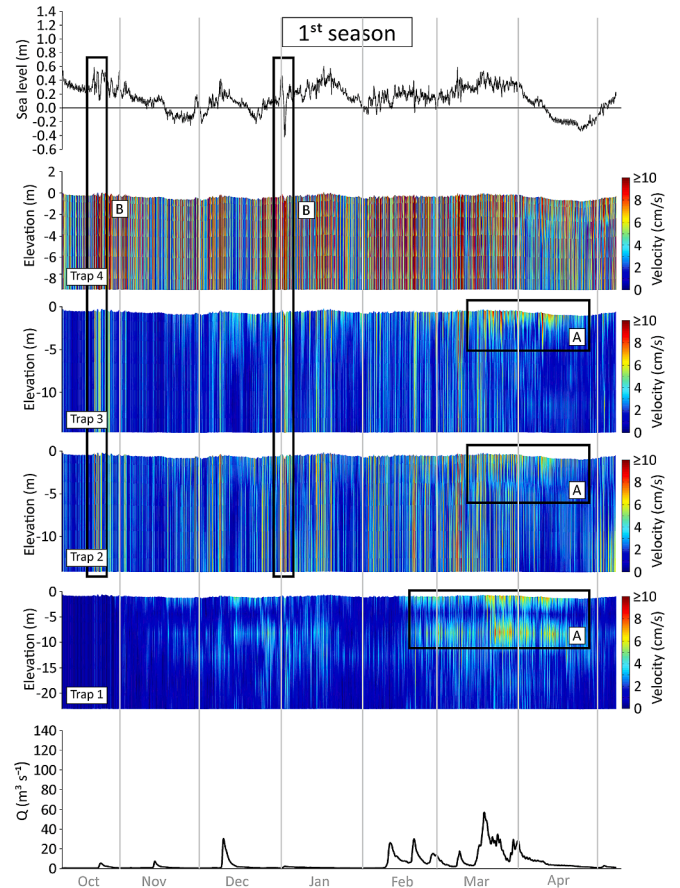


**Fig. 6.** The flow velocities of the first season in relation to sea level variation and discharge (Q) at each trap (see trap locations in Fig. 1). Velocity profiles consist of six vertical layers with 1-h intervals. Highlighted areas A and B are discussed in the text. Sea level values are heights in Baltic Sea Chart Datum.

and 0.35 (2nd season) between bottom flow velocities and sea level changes were found at trap 4.

#### 4.3. Sedimentation rate and characteristics

The average SAR along the bay area was nearly three times higher during the second than the first season,  $30.9$  and  $10.6 \text{ g m}^{-2} \text{ day}^{-1}$ , respectively (Table 1). During the second season, the SAR increased significantly at all traps: two to three times higher than the first season, and at trap 4, up to six times higher. Interestingly, SAR at trap 4 during the first season was similar to traps 1 and 3, but much higher during the second season.

The mean grain size ( $D_{50}$ ) was generally lower during the second season, except for trap 4 (Table 1). In both seasons, the mean grain size increased towards the sea, being much higher at trap 4.

While sediments of the first season had higher organic matter content, the total amount of organic matter accumulation was larger during the second season (Table 1). The organic matter content showed a decreasing trend from the river mouth towards the open sea. The total organic matter flux varied considerably between traps and was significantly larger during the second season. However, due to increased SAR and minerogenic flux, this was not seen in the organic matter content percentage (Table 1). C/N ratios were quite stable between the traps during the first season and showed more variability during the second season (Table 1). In general, C/N values were lower during the second season, except at trap 1. For both years, the C/N ratio was highest closer to the river mouth and at the deepest location. Total accumulation of N and C increased towards the open sea.

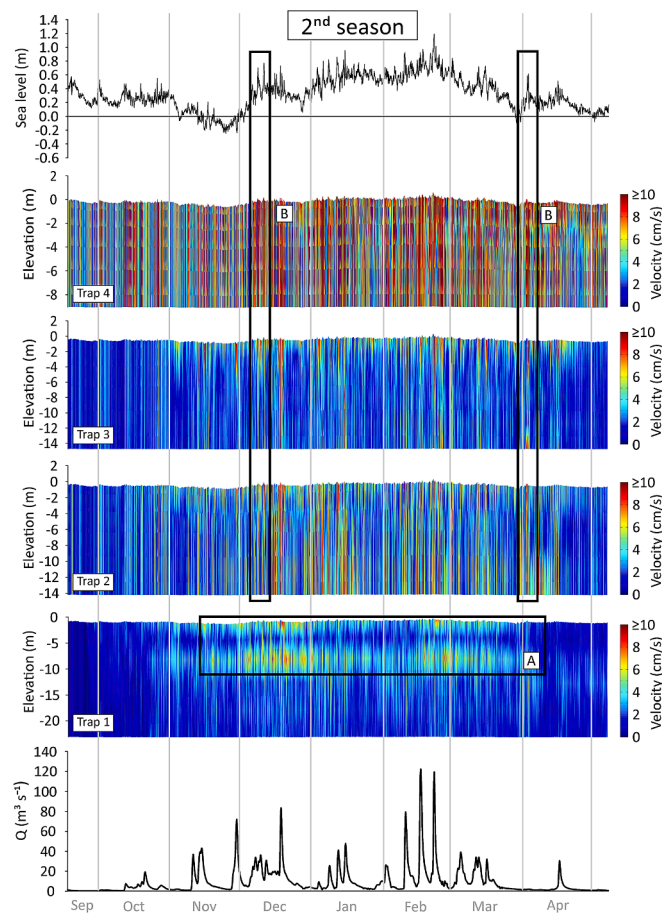


Fig. 7. The flow velocities of the second season in relation to sea level variation and discharge (Q) at each trap (see trap locations in Fig. 1). Velocity profiles consist of six vertical layers with 1-h intervals. Highlighted areas A and B are discussed in the text. Sea level values are heights in Baltic Sea Chart Datum.

Sediments consisted mostly of clastic matter (85–89%), for which the mean grain size varied from clay to fine silt (0.3–3.0 μm) (Table 1). The common feature between all the samples was that the grain size distribution was bimodal (Fig. 8) having peaks approximately at 0.2 and 3.0 μm grain size fractions.

## 5. Discussion

### 5.1. Hydrodynamic conditions

Our hydrodynamic models show that the high flow velocity events in the Halikonlahti Bay relate to river flow peaks and sea level changes. Usually, high river flows and rapid sea level changes occur simultaneously and are caused by low air pressure systems. A link between high river discharge events and high flow events could be seen only at trap 1, while in the rest of the traps, the high flow events are caused by the

combination of sea level changes and river flow.

The highest flow velocity events at traps 1–3 occurred simultaneously with high river discharge, caused mainly by snowmelt during the first year and high rainfall during the second year. These high flow velocity events are most likely related to the outflow of excess water from the bay towards the open sea (Salmela et al., 2020).

A two-layered velocity patterns found at trap 1 could relate to buoyant plume development along the bay, which in turn is found to produce positive estuary circulation (Salmela et al., 2020). In addition, the flow within the water column at traps 2–4 could be explained by the smaller water depth.

### 5.2. Sedimentation rate and characteristics between the seasons

A significant increase in SAR between the seasons suggests that snow- and ice-free conditions accompanied by higher precipitation and winds related to frequent low pressures, such as the second season, caused enhanced littoral resuspension and erosion on the catchment increasing the sediment load from land to estuary. The enhanced SARs during the second season is consistent with finding of Pruski and Nearing (2002) who stated that increased runoff in the catchment area increases soil erosion. Even though the fetch in the bay area is relatively small compared to open sea (Tolvanen and Suominen, 2005) previous studies highlight the importance of shoreline and bottom resuspension at shallow areas (Jokinen et al., 2015). In addition, during the second season, only 7% (48.9 mm) of the total precipitation was snowfall, which in turn increased rainfall erosivity and soil erosion. Moreover, the frost and snow cover during the first season might have reduced the rainfall erosivity by creating a protective layer against direct exposure to raindrops. This is in line with reduced catchment erosion during colder winters reported earlier from lake context (Saarni et al., 2016, 2017).

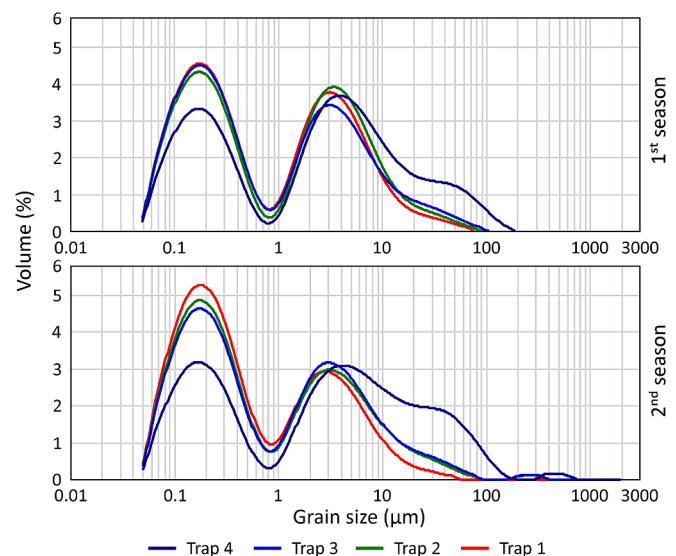


Fig. 8. Grain size distribution of the sediment samples for each trap during both seasons.

Table 2

Pearson correlations between sea level change, river discharge (Q) and flow conditions for both seasons. The highest correlations between the traps are bolded.

		Surface flow				Bottom flow			
		Trap				Trap			
		4	3	2	1	4	3	2	1
Sea level change	1st	<b>0.31</b>	0.07	0.14	−0.01	<b>0.34</b>	0.28	0.21	0.08
	2nd	<b>0.31</b>	0.09	0.19	0.12	<b>0.35</b>	0.30	0.23	0.14
Q	1st	0.09	0.35	0.28	<b>0.46</b>	0.08	0.14	0.07	<b>0.24</b>
	2nd	0.24	0.31	0.27	<b>0.39</b>	0.24	<b>0.27</b>	0.18	0.22

The second season was more active in terms of flow velocities, which seems to be related to higher river inflows and sea level changes. This could also explain high sedimentation difference between the two cold seasons as higher river flow increases river borne sediment load and higher flow velocities increase littoral resuspension potential. The highest flow velocities were mainly forced by rapid sea level changes, related to passages of low air pressure systems or seiches that are usually associated with sea level changes in the Baltic Sea region (Jakobsen et al., 2010; Jönsson et al., 2008). The lack of protective ice cover combined with higher wind speed and related wave activity as well as flow conditions during the second season likely increased shore erosion, littoral resuspension, and thus, sedimentation (Ryabchuk et al., 2011). In fact, the highest bottom and surface flow velocities were found at trap 4 during the second season, which could explain the six times larger SAR during the second season through enhances resuspension of littoral sediments in local surroundings.

Despite the highest flow velocities were also located at trap 4 during the first season, the SAR remain similar to traps 1 and 3. The SAR difference at trap 4 between the two seasons could be explained by the higher frequency of low air pressure system and thus sea level change-induced flows, combined with wave induced resuspension in open water conditions during the second season. In addition, the smallest cross-sectional area at trap 4, ca. 16% of the largest cross-sectional area of trap 1, induce highest flow velocities between the traps. Based on flow continuity, flow velocities become higher at smaller cross-sectional sites. For example, in channels with large quantities of water in adjoining water bodies, the flows are most likely forced by the sea level differences between the water bodies. In our study area, the sea level changes, during the passage of the low air pressure system, induce sea level slope between the open sea and bay area. This slope was shown as high flow velocities at the narrow channel area at trap 4. Furthermore, the effect of the sea level changes on flow velocities decreased towards inshore highlighting the effect of sea level change on flow velocities closer to the open sea. Moreover, the trap 4 is located closest to the shoreline compared to other traps, which might explain significantly higher sedimentation under open water conditions and frequent storm events due to nearshore wave induced littoral resuspension.

The higher organic matter content and C/N ratio closer to the river mouths during both seasons could be explained by riverine transport bringing more terrigenous organic material to the bay (Meyers and Ishiwatari, 1993) and increased carbon settling through flocculation of dissolved organic matter (Jilbert et al., 2018). Jähmlich et al. (2002) recorded similar values of C/N to ours, varying between 7.48 and 13.16 at the Oder River outlet of the southern Baltic Sea. Contrary to our findings, Jähmlich et al. (2002) found an increased C/N ratio towards offshore, which likely related to ageing of the material transported offshore.

The higher C/N ratio of the first season denotes a larger influence of terrigenous organic material transported from the catchment. The lower C/N ratio suggests enrichment of autochthonous organic matter that likely originated from resuspended littoral sediments. This finding is consistent with increased resuspension potential caused by open water, higher wind and flow conditions during the second season.

The difference in the mean grain size ( $D_{50}$ ) value between the seasons could be explained by higher settling on small particle sizes during the second season, thus decreasing the  $D_{50}$  value. Settling of the small particle size was likely related to the resuspension of littoral sediments and precipitation-induced sediment yield from the watershed during the second season. While for the first season, the catchment erosion was primarily characterised by the intensive snow melt-induced flow event, which in turn can cause movement of larger grains.

In both seasons, the mean grain size increased towards the sea being much higher at trap 4. The strongest flow velocities at trap 4 might explain the highest grain mean size in both seasons. In addition, our hydrodynamic model showed that the flow at trap 4 was mostly constant within the water column, which causes high near-bottom velocities

simultaneously with high surface velocities. Higher near-bottom flow velocities have been recorded as inducing higher resuspension of bottom sediments (Rasmus et al., 2015). Occasional high near-bottom flow events occurred at traps 2 and 3, but not at trap 1, where water is much deeper than at other trap locations.

Bimodal grain size distribution at each trap is likely a result of the two different sedimentation conditions within the seasons: a normal condition with low wind speed or ice cover enabled the accumulation of fine-grained matter while storm events, caused erosion on the littoral zone, and led to rapid accumulation of the larger particles (Jokinen et al., 2015). Likewise, snow melt-induced spring floods and high rainfall at the catchment increase transport and accumulation of the larger minerogenic fraction (Ojala et al., 2013). This is in line with the observed volume of 0.2  $\mu\text{m}$  grain size fraction, which was slightly larger during the second season with open water conditions, likely owing to reworking of the littoral sediments. The volume of 3.0  $\mu\text{m}$  grain size fraction is considerably larger during the first season, which was likely a result of rapid increase in catchment erosion and water flow during the short episode of spring floods. The larger 3.0  $\mu\text{m}$  fraction closer to the river mouth in the first season supports the terrestrial source and riverine transport during spring flooding. Such trends could not be seen in the second season's 3.0  $\mu\text{m}$  fraction. In the estuaries close to river mouths, riverine input can significantly influence the grain size distribution, while temporal variation in grain size in the coastal zone outside river mouths are mainly modified on wind stress and sea floor morphometry that influence bottom water energy (Ning et al., 2016).

The sediment data indicated that cold winter conditions, including frost, snow accumulation, and ice cover, led to short and punctuated catchment erosion during spring flood event, but a reduction in sedimentation under ice cover. On the contrary, warmer winters with open sea conditions and higher frequencies of low air pressure system/storms caused enhanced catchment erosion, from not only land but also via resuspension of littoral sediments. This finding is in agreement with studies conducted in lake environments, where higher sediment resuspension rates under open water than ice cover conditions were observed (Kleeberg et al., 2013; Niemistö and Horppila, 2007).

The second season represented an analogue for future normal cold season conditions, suggesting enhanced erosion and organic carbon transport from land to coastal areas. The enhanced organic carbon burial is related to expansion of dead zones, anoxic sea floor areas, due to oxygen consumption caused by degradation of organic matter, that in turn, leads to release of nutrients from the sediments, intensifying the vicious cycle of internal phosphorus loading (Jokinen et al., 2018). Following the more frequent open water conditions, bottom resuspension can be increased further contributing to internal loading and eutrophication, which is one of the biggest environmental alterations in the Baltic Sea. Furthermore, predicted future climate conditions suggest increased temperature and precipitation accompanied with decreased winter ice occurrence. As shown by our results, such conditions challenges current ecosystems not only by spread of anoxic dead zones but also due to decreased light penetration related to suspended sediment loads and eutrophication hence leading to further deterioration of coastal key fauna, such as *Fucus vesiculosus* and *Zostera marina*.

## 6. Conclusion

The seasonal records of bottom-mounted sediment traps were analysed together with hydrodynamic model to detect differences between two distinctive cold seasons within the Halikonlahti Bay of the Northern Baltic Sea. Sediment accumulation rate and characteristics were compared with hydrometeorological and hydrodynamic conditions. The following conclusions can be drawn:

- Clear differences in sediment accumulation rate of settled material between two distinctive cold seasons were observed. The average SAR was nearly three times higher during season characterised by



higher rainfall and discharge and a lack of snow and ice cover compared to cold season characterised by ice and snow cover.

- Increasing storm events in warmer climate with ice-free conditions enhance wind-induced resuspension and flow velocities resulting higher sedimentation in coastal areas.
- The minerogenic grain size showed a generally lower mean size ( $D_{50}$ ) during warmer cold season with higher precipitation, resuspension, flow conditions and river flow. Sediment grain size distribution was bimodal along the bay during the seasons, which was likely a result of the two different sedimentation conditions: i) a normal condition with low wind speed or ice cover enabled the accumulation of fine-grained matter and ii) higher energy conditions caused either by storm events with intensified precipitation and enhanced flow velocities and wave activity on the littoral zone or spring thaw induced catchment erosion combined with high river flow led to accumulation of the larger particles.
- Sediments of the colder ice-rich cold season were more organically rich, but the total amount of organic matter accumulation was smaller.
- Hydrodynamic modelling combined with sediment measurements improves the understanding of sedimentation processes in coastal areas by linking flow conditions with sediment data.

### Declaration of Competing Interest

The authors declare that they have no known competing financial interests or personal relationships that could have appeared to influence the work reported in this paper.

### Acknowledgement

This study was funded by the Doctoral Programme in Biology, Geography and Geology at the University of Turku, Academy of Finland (Grant no 321869) and Turku University Foundation. The authors thank the Finnish Environment Institute, Finnish Meteorological Institute, Finnish Transport Infrastructure Agency, and European Space Agency for data. The comments of two anonymous reviewers significantly improved the manuscript.

### References

- Chou, L.M., Yu, J.Y., Loh, T.L., 2004. Impacts of sedimentation on soft-bottom benthic communities in the southern islands of Singapore. *Hydrobiologia* 515, 91–106. <https://doi.org/10.1023/B:HYDR.0000027321.23230.2f>.
- Christiansen, C., Kunzendorf, H., Emeis, K.C., 2002. Temporal and spatial sedimentation rate variabilities in the Eastern Gotland Basin, the Baltic Sea. *Boreas* 31, 65–74. <https://doi.org/10.1111/j.1502-3885.2002.tb01056.x>.
- Chubarenko, B., Chechko, V., Kileso, A., Krek, E., Topchaya, V., 2019. Hydrological and sedimentation conditions in a non-tidal lagoon during ice coverage – the example of Vistula Lagoon in the Baltic Sea. *Estuar. Coast. Shelf Sci.* 216, 38–53. <https://doi.org/10.1016/j.ecss.2017.12.018>.
- Eckh ell, J., Jonsson, P., Meili, M., Carman, R., 2000. Storm influence on the accumulation and lamination of sediments in deep areas of the Northwestern Baltic proper. *Ambio* 29, 238–245. <https://doi.org/10.1579/0044-7447-29.4.238>.
- Eronen, M., Gl uckert, G., Hatakka, L., 2001. Rates of Holocene isostatic uplift and relative sea-level lowering of the Baltic in SW Finland based on studies on isolation contacts. *Boreas* 30, 17–30. <https://doi.org/10.1111/j.1502-3885.2001.tb00985.x>.
- Heiri, O., Lotter, A.F., Lemcke, G., 2001. Loss on ignition as a method for estimating organic and carbonate content in sediments: reproducibility and comparability of results. *J. Paleolimnol.* 25, 101–110. <https://doi.org/10.1023/A:1008119611481>.
- HERTTA database, 2021. Finnish Environment Institute SYKE. <https://www.p2.ymparis.to.fi/scripts/hearts/welcome.asp> accessed 20 September 2021.
- Horpilla, J., Niemist o, J., 2008. Horizontal and vertical variations in sedimentation and resuspension rates in a stratifying lake - Effects of internal seiches. *Sedimentology* 55, 1135–1144. <https://doi.org/10.1111/j.1365-3091.2007.00939.x>.
- J ahmlich, S., Lund-Hansen, L.C., Leipe, T., 2002. Enhanced settling velocities and vertical transport of particulate matter by aggregation in the benthic boundary layer. *Geogr. Tidsskr.* 102, 37–49. <https://doi.org/10.1080/00167223.2002.10649464>.
- Jakobsen, F., Hansen, I.S., Ottesen Hansen, N.E., Østrup-Rasmussen, F., 2010. Flow resistance in the Great Belt, the biggest strait between the North Sea and the Baltic Sea. *Estuar. Coast. Shelf Sci.* 87, 325–332. <https://doi.org/10.1016/j.ecss.2010.01.014>.
- Jevrejeva, S., Drabkin, V.V., Kostjukov, J., Lebedev, A.A., Lepp aranta, M., Mironov, Y.U., Schmelzer, N., Sztobryn, M., 2004. Baltic Sea ice seasons in the twentieth century. *Clim. Res.* 25, 217–227. <https://doi.org/10.3354/cr025217>.
- Jilbert, T., Asmala, E., Schr oder, C., Tiihonen, R., Myllykangas, J.P., Virtasalo, J.J., Kotilainen, A., Peltola, P., Ekholm, P., Hietanen, S., 2018. Impacts of flocculation on the distribution and diagenesis of iron in boreal estuarine sediments. *Biogeosciences* 15, 1243–1271. <https://doi.org/10.5194/bg-15-1243-2018>.
- Jokinen, S.A., Virtasalo, J.J., Kotilainen, A.T., Saarinen, T., 2015. Varve microfabric record of seasonal sedimentation and bottom flow-modulated mud deposition in the coastal northern Baltic Sea. *Mar. Geol.* 366, 79–96. <https://doi.org/10.1016/j.margeo.2015.05.003>.
- Jokinen, S.A., Virtasalo, J.J., Jilbert, T., Kaiser, J., Dellwig, O., Arz, H.W., H anninen, J., Arppe, L., Collander, M., Saarinen, T., 2018. A 1500-year multiproxy record of coastal hypoxia from the northern Baltic Sea indicates unprecedented deoxygenation over the 20th century. *Biogeosciences* 15, 3975–4001. <https://doi.org/10.5194/bg-15-3975-2018>.
- J onsson, B., D o s, K., Nycander, J., Lundberg, P., 2008. Standing waves in the Gulf of Finland and their relationship to the basin-wide Baltic seiches. *J. Geophys. Res.* Ocean. 113, 1–11. <https://doi.org/10.1029/2006JC003862>.
- Kankaanp a, H., Vallius, H., Sandman, O., Niemist o, L., 1997. Determination of recent sedimentation in the Gulf of Finland using  $^{137}\text{Cs}$ . *Oceanol. Acta* 20, 823–836.
- Kleeberg, A., Freidank, A., J ohnk, K., 2013. Effects of ice cover on sediment resuspension and phosphorus entrainment in shallow lakes: Combining in situ experiments and wind-wave modeling. *Limnol. Oceanogr.* 58, 1819–1833. <https://doi.org/10.4319/lo.2013.58.5.1819>.
- Lund-Hansen, L.C., Petersson, M., Nurjaya, W., 1999. Vertical sediment fluxes and wave-induced sediment resuspension in a shallow-water coastal lagoon laboratory of marine environmental science. *Estuaries* 22, 39–46.
- Merkouriadi, I., Lepp aranta, M., 2015. Influence of sea ice on the seasonal variability of hydrography and heat content in Tv arminne, Gulf of Finland. *Ann. Glaciol.* 56, 274–284. <https://doi.org/10.3189/2015AoG69A003>.
- Meyers, P.A., Ishiwatari, R., 1993. Lacustrine organic geochemistry—an overview of indicators of organic matter sources and diagenesis in lake sediments. *Org. Geochem.* 20, 867–900. [https://doi.org/10.1016/0146-6380\(93\)90100-P](https://doi.org/10.1016/0146-6380(93)90100-P).
- Niemist o, J.P., Horppila, J., 2007. The contribution of ice cover to sediment resuspension in a shallow temperate lake: possible effects of climate change on internal nutrient loading. *J. Environ. Qual.* 36, 1318–1323. <https://doi.org/10.2134/jeq2006.0487>.
- Ning, W., Tang, J., Filipsson, H.L., 2016. Long-term coastal openness variation and its impact on sediment grain-size distribution: a case study from the Baltic Sea. *Earth Surf. Dynam.* 4, 773–780. <https://doi.org/10.5194/esurf-4-773-2016>.
- Nuorteva, J., Kankaanp a, H.T., 2016. Relocation of soft mud deposits: an example from the Archipelago Sea, northern Baltic Sea. *Mar. Geol.* 380, 148–162. <https://doi.org/10.1016/j.margeo.2016.08.002>.
- Ojala, A.E.K., Kosonen, E., Weckstr om, J., Korkonen, S., Korhola, A., 2013. Seasonal formation of clastic-biogenic varves: the potential for palaeoenvironmental interpretations. *GFF* 135, 237–247. <https://doi.org/10.1080/11035897.2013.801925>.
- Pedersen, T.M., Gallegos, C.L., Nielsen, S.L., 2012. Influence of near-bottom resuspended sediment on benthic light availability. *Estuar. Coast. Shelf Sci.* 106, 93–101. <https://doi.org/10.1016/j.ecss.2012.04.027>.
- Pruski, F.F., Nearing, M.A., 2002. Runoff and soil-loss responses to changes in precipitation: a computer simulation study. *J. Soil Water Conserv.* 57, 7–16.
- Rasmus, K., Kiirikki, M., Lindfors, A., 2015. Long-term field measurements of turbidity and current speed in the Gulf of Finland leading to an estimate of natural resuspension of bottom sediment. *Boreal Environ. Res.* 20, 735–747.
- Ruosteenoja, K., Jylh a, K., 2007. Temperature and precipitation projections for Finland based on climate models employed in the IPCC 4th Assessment Report. In: *Third International Conference on Climate and Water*, Helsinki, Finland, pp. 3–6.
- Ryabchuk, D., Kolesov, A., Chubarenko, B., Spiridonov, M., Kurennoy, D., Soomere, T., 2011. Coastal erosion processes in the eastern Gulf of Finland and their links with geological and hydrometeorological factors. *Boreal Environ. Res.* 16, 117–137.
- Saarni, S., Muschiattiello, F., Weege, S., Brauer, A., Saarinen, T., 2016. A Late Holocene record of solar-forced atmospheric blocking variability over Northern Europe inferred from varved lake sediments of Lake Kuninkaisenlampi. *Quat. Sci. Rev.* 154, 100–110. <https://doi.org/10.1016/j.quascirev.2016.10.019>.
- Saarni, S., Lensu, A., Tammelin, M., Haltia, E., Saarinen, T., 2017. Winter climate signal in boreal clastic-biogenic varves: a comprehensive analysis of three arved records from 1850 to 1990 AD with meteorological and hydrological data from Eastern Finland. *GFF* 139, 314–326. <https://doi.org/10.1080/11035897.2017.1389984>.
- Salmela, J., Kasvi, E., Alho, P., 2020. River plume and sediment transport seasonality in a non-tidal semi-enclosed brackish water estuary of the Baltic Sea. *Estuar. Coast. Shelf Sci.* 245, 106986. <https://doi.org/10.1016/j.ecss.2020.106986>.
- Su plinska, M.M., Pietrzak-Flis, Z., 2008. Sedimentation rates and dating of bottom sediments in the Southern Baltic Sea region. *Nukleonika* 53, 105–111.
- Szmytkiewicz, A., Zalewska, T., 2014. Sediment deposition and accumulation rates determined by sediment trap and  $^{210}\text{Pb}$  isotope methods in the outer puck bay (Baltic Sea). *Oceanologia* 56, 85–106. <https://doi.org/10.5697/oc.56-1.085>.
- Tolvanen, H., Suominen, T., 2005. Quantification of openness and wave activity in archipelago environments. *Estuar. Coast. Shelf Sci.* 64, 436–446. <https://doi.org/10.1016/j.ecss.2005.03.001>.
- Veijalainen, N., Lotsari, E., Alho, P., Vehvil ainen, B., K ayh k o, J., 2010. National scale assessment of climate change impacts on flooding in Finland. *J. Hydrol.* 391, 333–350. <https://doi.org/10.1016/j.jhydrol.2010.07.035>.
- Vihma, T., Haapala, J., 2009. Geophysics of sea ice in the Baltic Sea: a review. *Prog. Oceanogr.* 80, 129–148. <https://doi.org/10.1016/j.pcean.2009.02.002>.